A R T I C L E

High tumor incidence and activation of the PI3K/AKT pathway in transgenic mice define AIB1 as an oncogene

Maria I. Torres-Arzayus,[1] Jaime Font de Mora,[1,4] Jing Yuan,[1] Francisca Vazquez,[1] Roderick Bronson,[2] Montserrat Rue,[3] William R. Sellers,[1] and Myles Brown[1,*]

[1]Division of Molecular and Cellular Oncology, Department of Medical Oncology, Dana-Farber Cancer Institute and Harvard Medical School, 44 Binney Street, Boston, Massachusetts 02115
[2]Department of Pathology, Harvard Medical School, 44 Binney Street, Boston, Massachusetts 02115
[3]Department of Biostatistical Science, Dana-Farber Cancer Institute, 44 Binney Street, Boston, Massachusetts 02115
[4]Present address: Fundación Valenciana de Investigaciones Biomédicas, Instituto de Investigaciones Citológicas, Valencia, Spain
*Correspondence: myles_brown@dfci.harvard.edu

Summary

The gene encoding AIB1, an estrogen receptor coactivator, is amplified in a subset of human breast cancers. Here we show that overexpression of AIB1 in transgenic mice (AIB1-tg) leads to mammary hypertrophy, hyperplasia, abnormal postweaning involution, and the development of malignant mammary tumors. Tumors are also increased in other organs, including the pituitary and uterus. AIB1 overexpression increases mammary IGF-I mRNA and serum IGF-I protein levels. In addition, IGF-I receptor and downstream signaling molecules are activated in primary mammary epithelial cells and mammary tumor cells derived from AIB1-tg mice. Knockdown of AIB1 expression in cultured AIB1-tg mammary tumor cells leads to reduced IGF-I mRNA levels and increased apoptosis, suggesting that an autocrine IGF-I loop underlies the mechanism of AIB1-induced oncogenesis.

Introduction

AIB1 was cloned from a region of chromosome 20q11-13 frequently found amplified in human breast and ovarian carcinomas (Anzick et al., 1997). AIB1 is a member of the p160 family of nuclear receptor coactivators (Halachmi et al., 1994), which also includes SRC-1 and SRC-2. These proteins significantly increase hormone-induced transcription mediated by nuclear receptors, such as estrogen receptor (ER), progesterone receptor (PR), thyroid hormone receptor (TR), glucocorticoid receptor (GR), and retinoic acid receptor (RAR), when overexpressed in the presence of ligand (reviewed in Glass and Rosenfeld, 2000; McKenna et al., 1999). Recently, we have shown that the recruitment of the p160 coactivators to the ER is a dynamic process sufficient for gene activation as well as cell cycle progression (Shang et al., 2000).

AIB1 function can be regulated by upstream signaling pathways, such as MAPK and IκB kinase (IKK), thus conveying growth factor and proliferation signals to the estrogen receptor (Font de Mora and Brown, 2000; Wu et al., 2002). AIB1 has also been shown to function in a hormone receptor-independent fashion to coactivate other p300/CBP associated transcription factors. For example, AIB1 can enhance transcription mediated by STAT and NF-κB (Torchia et al., 1997) and can reverse NF-κB-mediated inhibition of GR-activated genes (Werbajh et al., 2000).

Mice with a null mutation for the mouse homolog of AIB1, p/CIP, are dwarfed and show impaired morphogenesis of the mammary ductal system (Xu et al., 2000). This contrasts with the minimal effect of SRC-1 deletion on the mammary gland (Xu et al., 1998) and suggests that AIB1 may be a nuclear receptor coactivator critical for mammary gland development.

Thus far, AIB1 is the only p160 nuclear coactivator that has been linked to cancer. AIB1 mRNA levels were found to be increased in up to 60% of human breast tumors (Anzick et al., 1997), and AIB1 protein levels were reported to be higher in breast tumor sections as compared to normal breast tissue (List et al., 2001). AIB1 was also found to be amplified in hepatocellular carcinoma (HCC) (Wang et al., 2002), and in primary gastric cancers (Sakakura et al., 2000). In normal tissue, AIB1 is widely expressed with particularly high levels in testis, mammary gland, uterus, pituitary, heart, lung, liver, skeletal muscle, and brain (Chen et al., 1997; Takeshita et al., 1997; Torchia et al., 1997; Suen et al., 1998).

S I G N I F I C A N C E

AIB1, an estrogen receptor coactivator, has been implicated as a causal factor in human breast cancer, as its gene is amplified and/or overexpressed in a significant number of cases. We have tested this directly by making transgenic mice expressing AIB1 in the mammary gland. These mice develop mammary hyperplasia and mammary carcinomas. In addition, we find that AIB1 overexpression leads to increased levels of the growth factor IGF-I, suggesting that its mechanism of action involves the establishment of an autocrine IGF-I loop. This breast cancer model demonstrates that AIB1 is indeed an oncogene, and provides evidence that supports the development of targeted therapies that interfere with IGF-I signaling as an approach to the treatment of tumors dependent on AIB1.

The connection between AIB1 overexpression and the ERα status of breast tumors is still controversial. While one study found that AIB1 overexpression correlated with ERα and progesterone receptor (PR) expression in breast tumors and with tumor size (Bautista et al., 1998), two other studies found that AIB1 overexpression occurred more frequently in ERα- and PR-negative tumors and correlated with high levels of HER2/neu and p53 proteins (Bouras et al., 2001; Osborne et al., 2003). The latter studies suggest that AIB1 might correlate with the more aggressive, HER2/neu-positive tumor phenotype, and that it might be involved in tamoxifen resistance.

While these studies indicate that AIB1 is frequently overexpressed in mammary tumors, we are not aware of any direct evidence demonstrating a functional role of AIB1 in mammary tumor formation. To address this issue, we directed AIB1 expression to the mammary epithelium of mice. AIB1-tg mice displayed abnormal mammary gland development and developed mammary adenocarcinomas and a variety of other tumors with high frequency. Furthermore, AIB1-tg mice and tumors showed increased IGF-I levels and increased activation of the IGF-IR/PI3K/AKT pathway. Our data demonstrate that AIB1 is sufficient to cause the formation of mammary carcinomas and other tumors, and thus is able to act as an oncogene.

Results

Establishment of AIB1 tg mice and analysis of transgene expression

We generated 13 lines of transgenic mice expressing a human AIB1 cDNA gene under the transcriptional control of the mouse mammary tumor virus (MMTV) long terminal repeat (LTR) promoter/enhancer. Seven lines were then selected to generate homozygous females. AIB1 mRNA expression of the seven AIB1-tg lines was analyzed. Mammary glands from mature, virgin mice (7 weeks) showed consistently high levels of AIB1 expression in all 7 founder lines, with lines D3 and D5 showing the highest and D6 showing the lowest expression (Figure 1A). Primers used were specific for AIB1 and did not amplify the endogenous murine AIB1 (p/CIP) mRNA. Next, we tested a variety of organs for endogenous p/CIP and tg-AIB1 mRNA expression using quantitative real-time PCR and determined the increase of transgene over wt expression. The organs were derived from at least 10 different mice from 3 different lines. The highest fold increase of AIB1/pCIP expression was found in the mammary gland (7.6-fold), followed by the pituitary (5.2-fold), lung and uterus (3.3-fold each), liver (3.1-fold) and ovaries (2.8-fold) (Figure 1B). Endogenous p/CIP mRNA levels were not altered in the AIB1-tg mice as compared with wt (data not shown).

Next we analyzed AIB1 mRNA levels during mammary gland development in the 3 different AIB1-tg lines and compared them to endogenous p/CIP mRNA levels of wt mice by quantitative PCR. We found AIB1 mRNA levels to be 2.5- to 8-fold higher than p/CIP levels of wt mice, depending on the developmental stage (Figure 1C). Protein expression was established by Western blots and immunohistochemistry, using an AIB1 antibody that detects both human AIB1 and mouse p/CIP. In Western blots, AIB1-tg mammary glands taken from virgin animals, 1 day postpartum, or 4 days after onset of involution showed significantly higher AIB1 plus p/CIP levels as compared to samples from wt animals (Figure 1D). Immunohistochemical analysis

showed that the strongest expression of AIB1 occurs in epithelial cells. Again, AIB1-tg mice consistently showed higher levels of AIB1 plus p/CIP expression as compared with wt animals during different stages of mammary gland development (Figure 1E).

Increased size of mammary gland, starting at 4 weeks of age

The sizes of virgin AIB1-tg mammary glands were measured as whole mounts and were found to be 30% to 40% larger as compared to wt mice (Figure 2A). The increased size of the mammary gland was already apparent at puberty (4 weeks of age). The increased mammary gland size in AIB1-tg mice seemed to be not only due to an increased number of epithelial cells but also due to an increased size of each individual cell.

Hyperplasia and accelerated differentiation of mammary gland in AIB1-tg mice during pregnancy

Whole-mount mammary glands from AIB1-tg mice at 2 weeks of pregnancy showed more extensive lobuloalveolar development, in contrast to pregnant wt animals. Moreover, mammary glands from AIB1-tg pregnant mice showed a more extensive degree of ductal branching as compared to wt mice (not shown). Histological sections of paraffin-embedded mammary glands of AIB1-tg mice at 1 day postpartum revealed a disorganized epithelium with respect to the columnar arrangement of a normal mammary epithelium (Figure 2B, top and bottom left panels). Animals from all founder lines showed this phenotype with high penetrance. In spite of the abnormal structure of the mammary gland at this stage, AIB1-tg mice were able to nurse their pups normally.

Delayed involution in AIB1-tg mice

Hematoxylin and eosin (H&E)-stained sections at day 4 after initiation of involution showed that the mammary alveolar structures from wt mice had started to collapse, and numerous apoptotic bodies were apparent in the luminal cells. In contrast, in mammary glands from AIB1-tg mice, the alveoli had not yet begun to collapse (Figure 2B, 4d inv. panels). At day 14 of involution, wt mammary glands were largely remodeled and resembled those of early pregnancy. In contrast, mammary glands from AIB1-tg mice were still undergoing involution, as was apparent from the collapsing alveolar structures and the disorganization of the gland (Figure 2B, 14d inv. panels). After 21 days of involution, wt mammary glands were completely remodeled, resembling the prepregnant state, while ducts from AIB1-tg mammary glands failed to remodel. Instead, they remained hypercellular, became dilated, and filled with secretions (Figure 2B, 21d inv. panels). These abnormalities persisted for at least several months following weaning.

Analysis of cell growth, proliferation, and apoptosis

The size of an organ is determined by coordinated regulation of cell growth (increase in cell size), cell proliferation (increase in cell number), and cell death (apoptosis) (Conlon and Raff, 1999). To determine the reasons behind the increased mammary gland size and hyperplasia observed in the AIB1-tg mice, we analyzed cell size, cell number, proliferation, and apoptosis in mammary gland epithelial cells of wt and AIB1-tg mice.

The size of the epithelial cells was measured in mammary glands from mice at day 1 postpartum, when we observed the
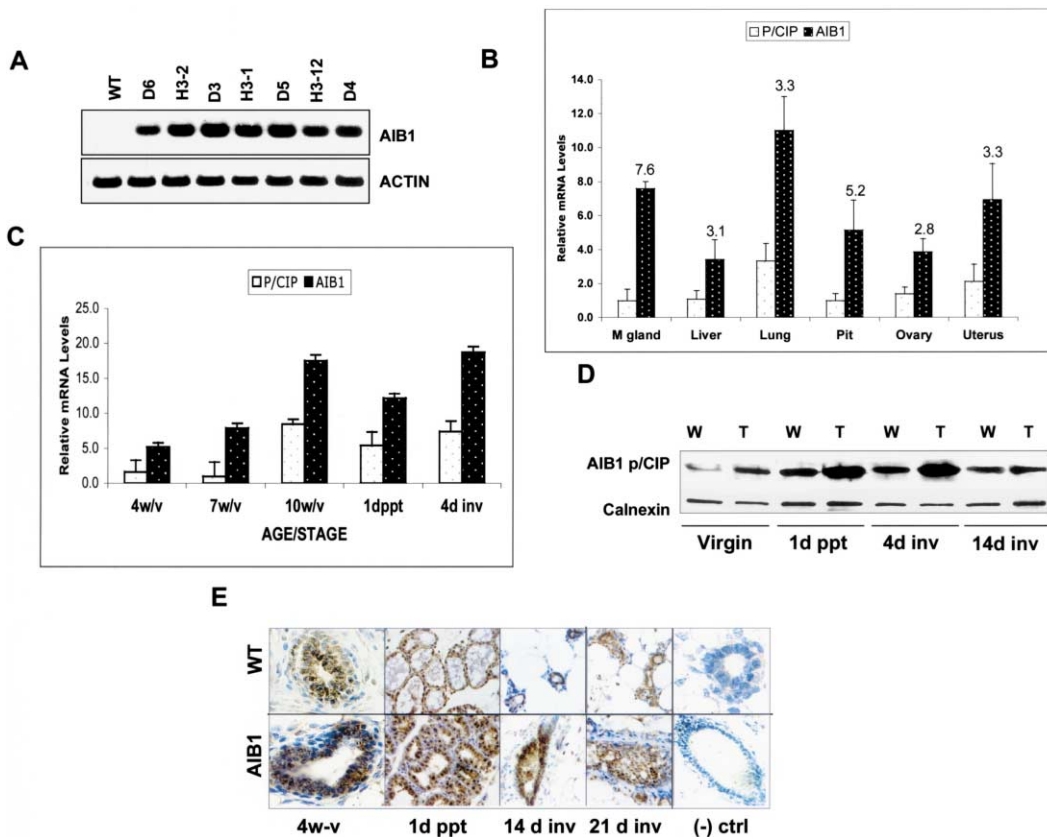
Figure 1. Expression pattern of the AIB1 transgene in mammary glands and different organs at different stages of development

A: AIB1 mRNA levels in different tg lines were determined by RT-PCR of total RNA from mammary glands of wt and tg mice, using primers specific for human AIB1.

B: AIB1 and endogenous p/CIP mRNA levels were determined in different organs of tg animals using real-time PCR with primers specific for p/CIP or AIB1. Results were normalized with GAPDH and averaged for 5 different experiments. The fold increase of tg over wt expression is indicated on top of each bar.

C: Real-time PCR analysis of ectopic AIB1 and endogenous p/CIP mRNA was performed on total RNA from wt and tg mammary glands at the indicated stages of development. p/CIP levels were determined in samples from wt mice, AIB1 levels in samples from tg mice. Experiments were performed in duplicates and repeated at least three times. Results were normalized with GAPDH.

D: Western blot analysis was performed to determine the combined protein levels of AIB1 and p/CIP in mammary glands from wt and AIB1 mice, at the indicated stages of development. Blots were reprobed with an anti-calnexin antibody to normalize for loading differences.

E: Immunohistochemical analysis was performed on sections of paraffin-embedded mammary glands from wt and tg animals. Sections were stained with a rabbit anti-human AIB1 primary antibody, developed with Vectastain ABC kit, and counterstained with hematoxylin. For the negative control, the primary antibody was omitted. W, week; d, day; v, virgin; ppt, postpartum; inv, involution.

greatest difference in size between wt and AIB1-tg mammary gland epithelial cells (Figure 3A). The average luminal epithelial cell diameter from AIB1-tg mice was 2.0-fold $\pm$ 0.2 (SD) larger than that of wt mice (Figure 3B). To quantify the ductal epithelial hyperplasia observed after onset of involution (see, for example, Figure 1E), we quantified epithelial cells at 21 days after initiation of involution. The epithelial cell number per area in the AIB1-tg mammary gland was determined to be 2.5-fold higher than that of wt animals (data not shown). BrdU analysis was performed on sections of mammary glands at 2 weeks of pregnancy, the stage of the maximal rate of epithelial cell proliferation. As shown in Figures 3C and 3D, the fraction of BrdU positive epithelial cells was ~50% higher in the AIB1-tg mammary gland as compared to the wt. TUNEL assays were performed on sections of mammary glands from day 4 after the onset of involution. As shown in Figure 3E, the number of epithelial cells undergoing apoptosis in the mammary glands of AIB1-tg mice was ~33% lower as compared to wt mice.

Analysis of serum levels of prolactin, luteinizing hormone, and growth hormone

In the course of this study, several mice developed pituitary tumors (see below). To examine the possibility that a change in serum levels of pituitary hormones, such as prolactin (PRL), luteinizing hormone (LH), or growth hormone (GH), was potentially responsible for the observed mammary gland phenotype, serum levels of these hormones were determined by radioimmunoassay (RIA) (Fedele et al., 2002). Serum levels from a total of 70 mice were examined, including wt and AIB1-tg animals, both male and female animals, and several animals with pituitary tumors. In all animals, serum levels of GH, PRL, and LH were within the physiological range and thus did not differ significantly between wt and AIB1-tg animals as a consequence of AIB1 overexpression (data not shown). Furthermore, animals were fertile and cycled normally. Therefore, the observed AIB1-tg phenotype of lobuloalveolar hyperplasia and accelerated differ-
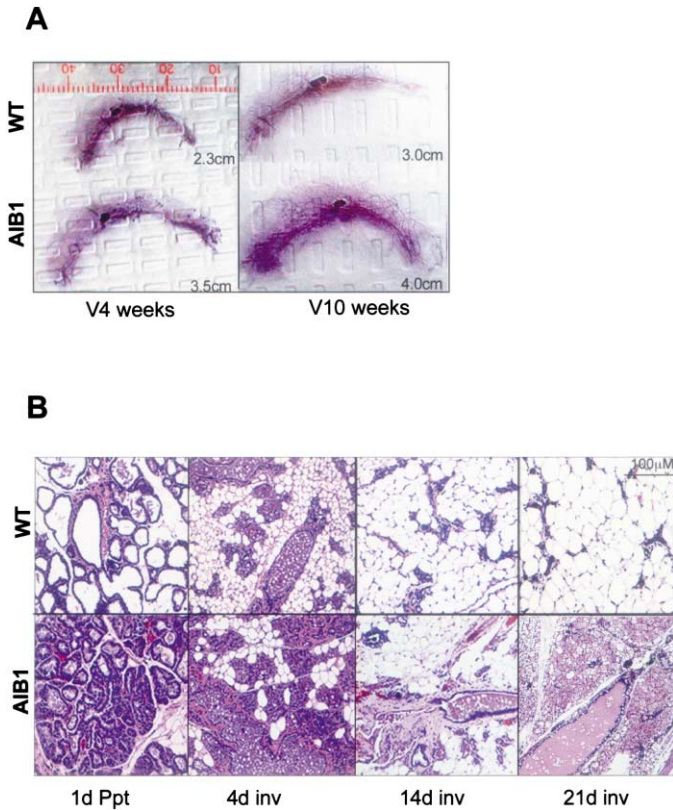
Figure 2. Increased mammary gland size, increased numbers of mammary gland epithelial cells, and disorganized mammary gland structure in AIB1-tg mice

A: Whole-mount photography of mammary glands from wt (top panels) and AIB1-tg mice (bottom panels) of 4-week-old (left panels) or 10-week-old (right panels) virgin mice. The respective length of the mammary glands in cm is indicated.

B: Histological analysis of H&E-stained mammary gland sections at different stages of development. Top panels show wt mammary glands. Bottom panels show AIB1-tg mammary glands.

entiation does not appear to result from differences in the levels of circulating PRL, GH, or LH.

Histopathological analysis of early proliferative lesions

Mammary glands of AIB1-tg mice showed numerous hyperplastic, noninvasive focal lesions, observed as early as 5 months of age. The hyperplastic lesions were multilayered and often appeared to be originating from ducts (Figure 4A). Solid lesions generally contained larger foci with dense masses of atypical cells organized in nodular sheets (Figure 4B). This phenotype developed in AIB1-tg mice independent of their reproductive history and without hormonal manipulation. The phenotype of these lesions is consistent with a premalignant phenotype, referred to as mammary intraepithelial neoplasia (MIN) (Cardiff et al., 2000). In addition to the hyperplastic structures, alterations of the lobular architecture were frequently observed in virgin and resting mammary glands, including differentiating alveoli and secretory alveolar structures (Figure 4C). Ductal ectasia and increased connective tissue was a particularly common feature in AIB1-tg mice (Figures 4B and 4C). Squamous metaplasia and

unusual squamous cysts with central keratin debris were also frequently observed in AIB1-tg mice (Figures 4D–4F).

Tumor incidence and analysis of tumor phenotype

In order to evaluate tumor incidence and age of onset, 203 tg mice from the seven founder lines were analyzed, and 100 mice were maintained for aging. Tumors developed in mice from all lines, and there was no correlation between tumor type and founder line. Mice were grouped by status as nulliparous (virgin) and parous (one or more litters). From the aging group of mice, 76 animals carrying 1 or several tumors were detected as early as 9 months of age, with an average latency of 16 months (Figure 5). In a total of 145 tumors, we detected a large number of mammary gland adenocarcinomas, pituitary adenomas, uterine leiomyosarcomas, and lung adenocarcinomas. Several other tumor types occurred with lesser frequency (Table 1).

In comparison, cohorts of age-matched wt controls (a total of 105 animals) only displayed 5 tumors (3 lung and 2 pituitary tumors) by 19–22 months of age. Significantly, none of the control animals developed mammary gland tumors. Both the rate of total tumor formation and the incidence of mammary gland tumors alone were significantly different between AIB1-tg and wt control animals ($p = 0.0007$ and $p = 0.0001$, respectively; Figures 5A and 5B). Thus, tumor formation in our model was strictly dependent on the transgene and could not be explained by the spontaneous formation of pituitary adenomas and associated mammary tumors reported for the strain of FVB/NCr mice (Wakefield et al., 2003). Furthermore, in our model, there was no correlation between the formation of pituitary adenomas and mammary tumors. Only a subgroup of mice developing pituitary adenomas showed mammary gland carcinomas, and vice versa, not all mice carrying mammary carcinomas developed pituitary adenomas. Interestingly, the frequency and latency of mammary tumorigenesis in nulliparous AIB1-tg mice was not significantly different from that of the parous studied mice (Figure 5D and log-rank test; data not shown), suggesting that the tumorigenicity of AIB1 is independent of the reproductive history of the mice.

The histopathology of the mammary tumors revealed an incidence of several subtypes of adenocarcinomas (Figure 5E, top panels), including acinar, ductal, solid comedo type, and papillary adenocarcinoma as defined by the Annapolis Histopathology Conference (Cardiff et al., 2000). Most of the tumors were invasive, as determined by the presence of nests and cords of tumor cells infiltrating the adjacent tissue like skeletal muscle or brain (as in the case of some pituitary tumors). Furthermore, several adenocarcinomas were metastatic, showing tumor formation composed by the same original cell type in lung, bones, and kidney (not shown).

Analysis of AIB1 and ERα expression in mammary gland tumors

We analyzed the AIB1 and ERα expression status of mammary gland tumors from AIB1-tg mice by immunohistochemistry, Western blot, and quantitative PCR. By immunohistochemistry, approximately 85% of the tumors were ER-positive with nuclear staining, while 15% of the mammary gland tumors were ER-negative (Figure 5E). Tumors were considered ER-positive when more than 1% of the tumor cells showed ER staining regardless the intensity of staining. An example of a tumor scored as ER-negative tumor can be seen in Figure 5E. In this tumor, the malignant cells are ER-negative, while areas of normal epithelial
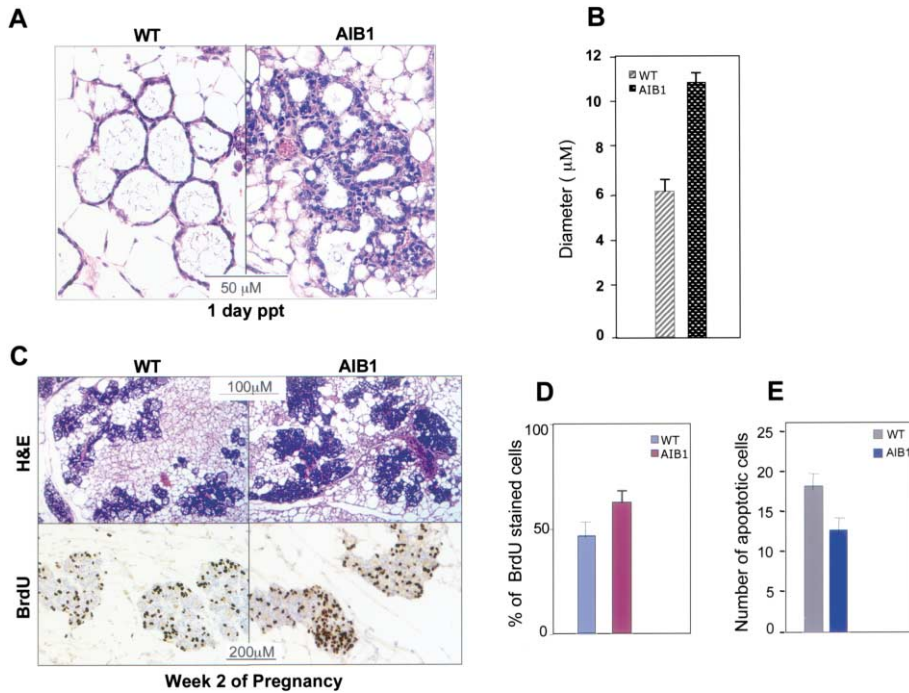
Figure 3. Increased cell growth, increased proliferation, and delayed apoptosis in AIB1-tg mammary glands

A: The average cell size was determined from wt and AIB1-tg mice at 1 day postpartum by measuring the maximum diameter of epithelial cells in histological cross-sections.

B: For each mammary gland, a total of 500 cells in 10 different fields were measured and the average diameter calculated. Similar results were obtained from at least 5 mammary glands.

C and D: Determination of the number of proliferating cells by BrdU incorporation. Wt (left panels) and AIB1-tg (right panels) mice at 2 weeks of pregnancy were injected with BrdU. Cross-sections of isolated mammary glands were stained with H&E (upper panel) or with an anti BrdU antibody followed by counterstaining with hematoxylin (lower panel) **(C)**. The number of BrdU-positive cells was counted in 10 fields per slide. Graphed results represent the average of 3 independent assays **(D)**.

E: Determination of the number of apoptotic cells by TUNEL assay. After TUNEL labeling, the number of dUTP-positive cells was determined in mammary glands from mice 4 days after initiation of involution. Graphed results represent the average of 3 independent assays.
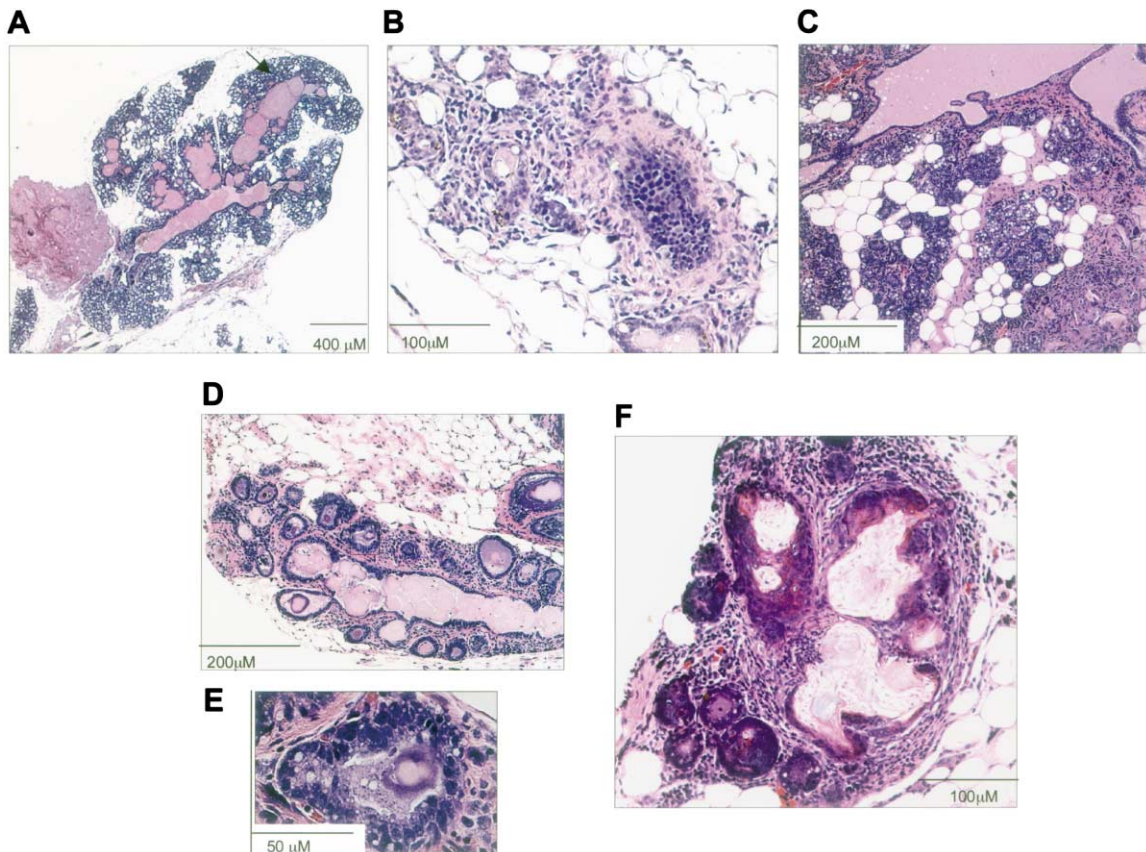

Figure 4. Histological analysis by H&E staining reveals premalignant phenotype of AIB1-tg mammary glands

A: Example of persistent hyperplasia and ductal ectasia in a nulliparous AIB1-tg mouse.
B: Example of a solid lesion with dense masses of atypical cells surrounded by connective tissue.
C: Secreting alveolar structures are surrounded by stromal tissue in the mammary gland of nulliparous tg mice.
D–F: Squamous metaplasia and unusual squamous cysts, shown at different magnifications.
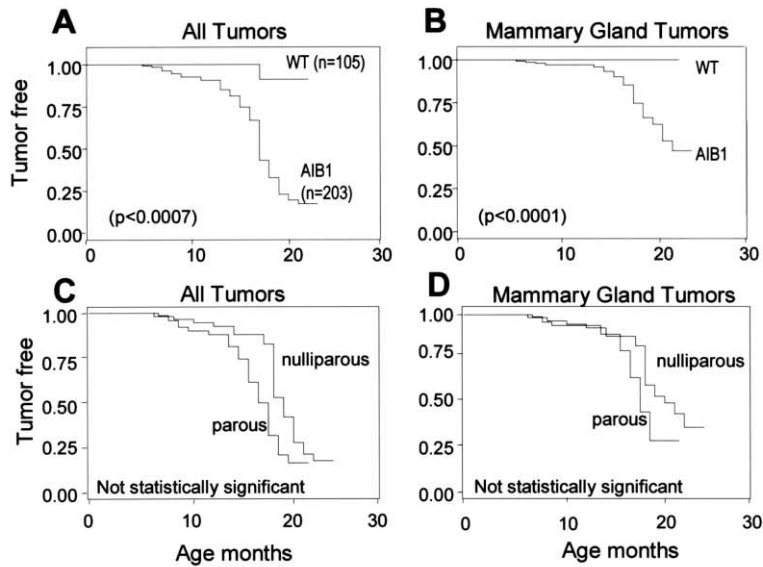
Figure 5. Tumor-free survival of mice and histo-pathological and immunohistochemical analysis of mammary adenocarcinomas

A and B: Kaplan-Meier analysis of tumor-free survival of wt versus AIB1-tg mice. **A:** Tumors of all origins were taken into account. **B:** Only mammary tumors were taken into account.

C and D: Kaplan-Meier analysis of tumor-free survival of nulliparous versus parous AIB1-tg mice, accounting for all tumors (**C**) or mammary tumors only (**D**). The median of tumor incidence for all tumors was 16 months.

E: Paraffin-embedded sections of tumors were stained with H&E (top panels), anti-AIB1 antibody (middle panels), or anti-ERα antibody (lower panels). Tumors represented lobular, microacinar, and comedo type. The arrow in the lower left panel indicates ER staining of normal cells. Tg lines from which the tumors were obtained are indicated below.
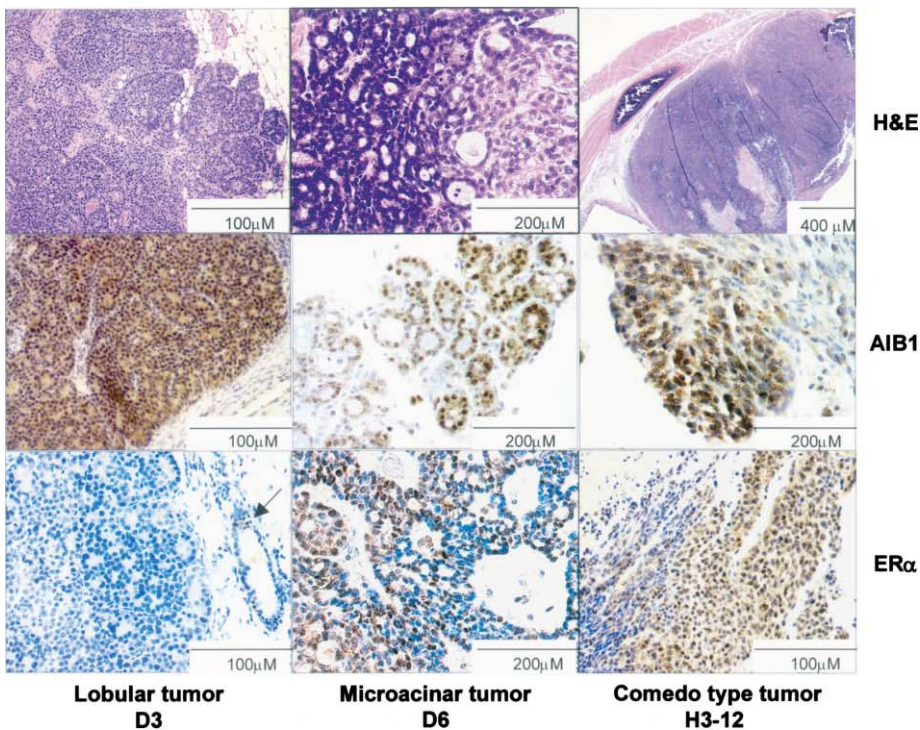
cells demonstrate normal ER staining. Interestingly, while AIB1 was strongly expressed in normal, hyperplastic, and malignant epithelial cells, its localization, while nuclear in the normal epithelium, was often cytoplasmic in tumor cells (Figures 1E and 5E).

Activation of the IGF-R/PI3K/AKT/mTOR pathway and GSK3 in mammary glands and tumors from AIB1-tg mice

Increased cell and organ sizes have been linked to upregulation of the PI3 kinase/AKT/mTOR pathway (Patel et al., 2002; Leevers et al., 1996). We therefore determined whether this pathway is activated in mammary glands and tumors of AIB1-tg mice by probing Western blots with antibodies for phosphorylated forms of a comprehensive set of members of this signaling pathway, including pIGF-IR (tyr1131), pAKT (ser473), pTSC (thr1462), pmTOR (ser2448), peIF4G (ser1108), pp70S6K (thr389), and pS6RP (ser235/236).

First, we analyzed extracts from whole mammary glands at different stages of development (Figure 6A). Differences in p70S6K and S6RP phosphorylation between wt and AIB1-tg mammary glands were already apparent at 7 weeks of age. Phosphorylation of these proteins increased dramatically in the

Table 1. AIB1 tumor incidence

Tumor type	Number
Mammary gland adenocarcinomas	48
ERα (+) mammary gland tumors	40
ERα (−) mammary gland tumors	8
Pituitary adenomas	42
Uterine leiomyosarcomas	18
Lung adenocarcinomas	18
Fibrosarcomas	6
Skin papillomas	3
Ovarian teratomas	3
Lymphomas	2
Osteomacrophage sarcomas (liver)	2
Adrenocortical tumors (kidney)	2
Squamous cell carcinoma (skin)	1
Total tumors	145
Animals bearing tumors	76
Total aging animals	100

course of pregnancy, in both wt and AIB1-tg animals and in parallel with AIB1 levels. While p-S6RP levels decreased in AIB1-tg and wt animals during involution, p-p85S6K levels remained high in AIB1-tg animals and only declined in wt animals.

We next wanted to examine whether the increased levels of these phosphoisoforms were indeed occurring in AIB1-over-expressing epithelial cells or whether there was any involvement of stroma cells in this upregulation. We generated primary epithelial cell cultures (ECC) from virgin wt and AIB1-tg mammary glands of 10-week-old mice and examined protein extracts. All phosphoisoforms examined were found to be increased between 3- and 20-fold in ECC from AIB1-tg mammary glands (Figure 6B). In contrast, the nonphosphorylated forms of the proteins examined remained largely unchanged, with the exception of mTOR, which also showed a strong increase in expression in the AIB1-tg samples. In addition to these factors, we examined another target of AKT, GSK3β (ser9), and one of its downstream effectors, cyclin D1. Among other functions, GSK3β is implicated in the activation of β-catenin. Phosphorylation of Ser 9 of GSK3β, the substrate of AKT, was strongly increased in AIB1-tg ECC samples, while total GSK3β levels remained constant. Furthermore, cyclin D1 levels were dramatically increased and pβ-catenin (ser45) levels decreased in the AIB1-tg ECC (Figure 6B and data not shown). This pβ-catenin is targeted for degradation by the proteasome, while unphosphorylated β-catenin accumulates and translocates to the nucleus, leading to the activation of target genes. We also analyzed
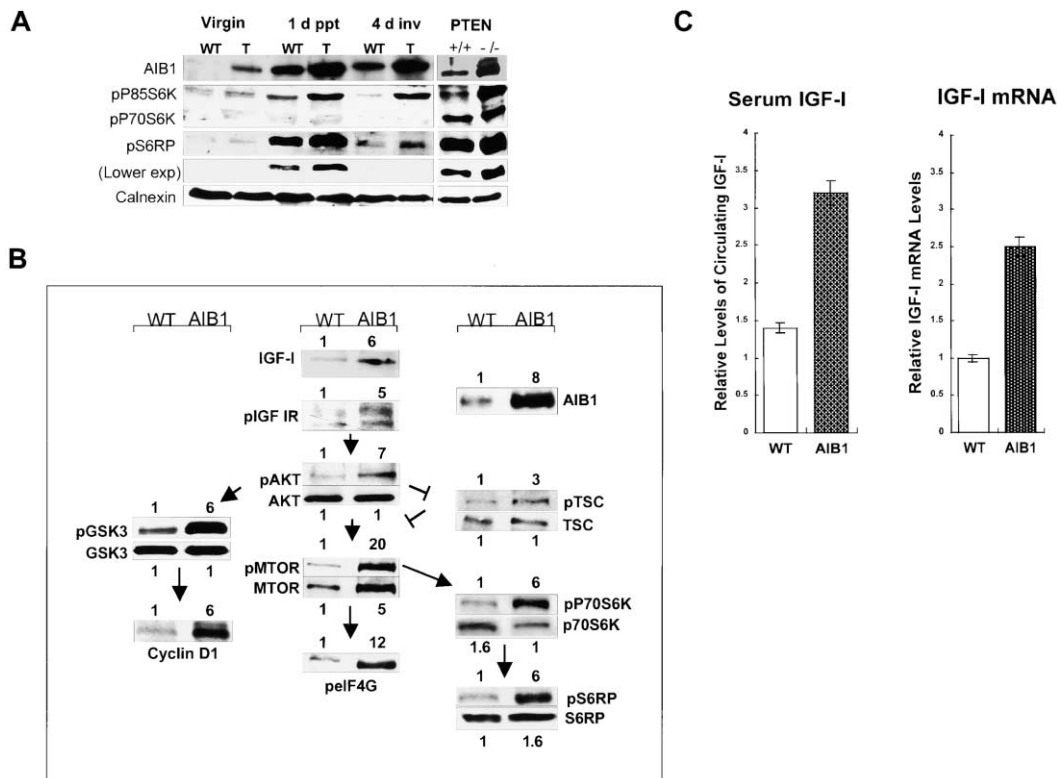
Figure 6. AIB1 activates the PI3K/AKT/mTOR pathway and its downstream effectors

A: Western blot analysis of mammary gland extracts from different stages of development. Mouse embryo fibroblasts from PTEN null mutants (−/−) and wt mice (+/+) served as controls for the activation of the PI3K/AKT pathway.

B: Western blot analysis of 40 μg protein extracts from ECC of 10-week-old wt and AIB1-tg mice, using phospho-antibodies (p) and total levels of the indicated proteins. Signal intensities were determined by densitometry and normalized using a calnexin antibody.

C: Analysis of IGF-I serum levels by IP-Western blot (left panel) and IGF-I mRNA levels in primary ECC by quantitative RT-PCR (right panel). 250 μl of serum from 10-week-old AIB1-tg or wt mice was subjected to immunoprecipitation and subsequent Western blot analysis using IGF-I antibody. Band intensities were determined by densitometry and averaged over 3 independent experiments (left panel). Total RNA from primary ECC derived from 10 tg and 10 wt control mice was quantified by real-time PCR, using IGF-I specific primers.

protein extracts from primary mammary tumors and tumor-derived cell lines. All samples analyzed showed similarly high levels of the phosphorylated forms of IGF-IR, p70S6K, and pS6RP (data not shown).

Since IGF-IR was found to be activated in AIB1 tumors as well as in mammary glands and primary ECC of AIB1-tg mice, we wanted to determine whether AIB1 might activate IGF-IR through an increased production of IGF-I. We therefore measured IGF-I serum levels and levels of IGF-I protein and mRNA in the mammary gland. We found circulating IGF-I levels to be increased by ~2.5-fold in AIB1-tg as compared with wt animals. A similar increase was detected for IGF-I mRNA levels in AIB1-Tg ECC (Figure 6C).

PR levels are downregulated in tg mammary glands and ECC despite increased ERα levels

It has been shown that increased IGF-I levels lead to lower progesterone receptor (PR) mRNA and protein levels in breast cancer cells (Cui et al., 2003a, 2003b). Consistent with these data, we found PR levels to be lower in AIB1-tg mice, as early as 10 weeks of age (as determined by Western blot, data not shown). In contrast, ERα levels were found to be persistently higher in AIB1-tg as compared to wt mammary glands. Thus, PR expression is regulated independently from ERα expression in AIB1-tg.

AIB1 silencing demonstrates its necessity in IGF-I expression and cell survival

The phenotypic changes observed in AIB1-tg mice might be triggered by AIB1 in an indirect manner through early events in the life of an AIB1-tg mouse. In this case, AIB1 might no longer play a direct role in the maintenance of a hyperplastic or tumoro-genic phenotype of the mammary gland. Alternatively, AIB1 may continue to play a critical role after the phenotypic changes occur. To distinguish between these possibilities, we knocked down AIB1 expression in cell lines derived from AIB1-tg prema-lignant mammary glands and tumors using siRNA, and deter-mined the phenotypic changes of these cells. Western blot dem-onstrated that transfection with a specific AIB1 siRNA led to knockdown of AIB1 by >80% at protein level as compared to a nonspecific control siRNA (Figure 7A). In order to determine whether continued AIB1 expression is required for the increased level of IGF-I expressed in AIB1-tg ECC and tumor cells, we assayed the level of IGF-1 mRNA expressed in these cells fol-lowing knockdown of AIB1. The levels of IGF-I mRNA were decreased by ~66% in AIB1-tg ECC and ~50% in an AIB1-tg derived mammary tumor cell line 48 hr after AIB1-specific siRNA transfection (Figure 7B). These results demonstrate that contin-ued AIB1 expression is required to drive the high level of IGF-I expression found in these cells. Furthermore, FACS analysis revealed that 12 ± 3% of the AIB1 siRNA transfected cells were in the sub-GI fraction (Figure 7D), as compared to 0% for the mock transfected and 1% for control nonspecific siRNA trans-fected cells. TUNEL assay confirmed the marked increase in apoptosis in AIB1 siRNA transfected cells (Figure 7E). These data demonstrate that AIB1 is not only sufficient to induce mam-mary tumors, but also necessary for continued mammary tumor cell survival.

Discussion

Despite the circumstantial evidence linking AIB1 to human breast cancer, the role of AIB1 in the etiology of mammary carcinomas has not yet been rigorously established. Our study now demonstrates the potential of the AIB1 gene by itself to trigger a uniform premalignant phenotype in mammary epithelial cells that progresses with high frequency to mammary adeno-carcinomas.

Expression of the AIB1 transgene in our study was controlled by the MMTV LTR, the most frequently used promoter in tg models of mouse mammary cancer (Cardiff et al., 2000). The MMTV LTR has been shown to be active throughout mammary gland development, leading to particularly high expression dur-ing pregnancy and lactation (Gunzburg and Salmons, 1992). Consistent with these reports, we found that AIB1 transgene expression was already apparent in mature, virgin animals and persisted throughout cycles of pregnancy. However, MMTV LTR activity is not restricted to the mammary gland, but has also been reported for salivary glands, liver, lung, lymphoid cells, spleen, seminal vesicles, and testes, albeit at lower levels (Choi et al., 1987; King and Corley, 1990). In our study, we detected particularly high AIB1 expression levels in the lung, pituitary, and uterus, consistent with the development of tumors in these organs.

The somewhat different pattern of MMTV-LTR activity and AIB1 transgene expression reported here is not unexpected. First, the AIB1 transgene can function as a nuclear receptor coactivator for GR and PR (Liao et al., 2002), and glucocorticoids and progestins are the major activators of the hormone response elements present in the MMTV LTR (Gunzburg and Salmons, 1992). Second, AIB1 has been shown to function as an NF-κB coactivator (Torchia et al., 1997) and is able to counteract the NF-κB-mediated repression of GR (Scheinman et al., 1995). Thus, we would expect an MMTV-driven AIB1 transgene to undergo a significant degree of positive autoregulation. To our knowledge, MMTV LTR activity in the pituitary has not been previously reported, but it is not unexpected, given that MMTV expression is strongly activated by prolactin, a hormone pro-duced in the pituitary (Munoz and Bolander, 1989; Gunzburg and Salmons, 1992). The somewhat expanded activity of the MMTV LTR reported in this study enabled the unexpected dis-covery that AIB1 can mediate tumorigenicity in organs other than the mammary gland, most notably pituitary, lung, and uterus, and in tissues other than epithelial cells.

The mammary glands of a large majority of transgenic ani-mals from all seven founder lines showed a uniform premalig-nant phenotype. This phenotype consisted of an increased size of mammary glands and mammary gland epithelial cells, a failure to undergo complete involution, and the presence of squamous metaplasia, persistent hyperplasia, and continuously secreting glands (galactorrhea). We further showed that the persistent hyperplasia was due to a combination of increased cellular pro-liferation and evasion of apoptosis.

The AIB1-induced hyperplastic lesions observed appeared to be mainly alveolar lesions. The high-grade lesions showed several layers of epithelium, pleomorphism of nuclei, and an increase in mitotic figures, which are all hallmarks of mammary intraepithelial neoplasia (MIN). MIN lesions represent a morpho-logical intermediate between normal tissue and cancerous tis-sue and are considered to have a high potential for malignancy
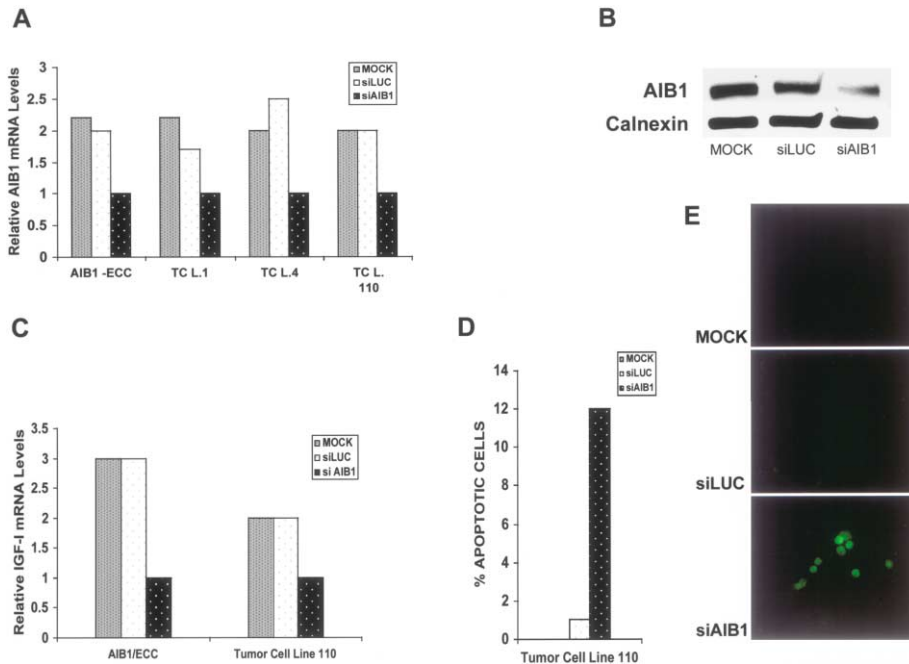
Figure 7. Silencing of AIB1 expression leads to reduction of IGF-I levels and to apoptosis

A and B: Primary ECC and tumor cell lines (TCL1, TCL4, TCL110) from AIB1-tgs were transfected with siRNA oligos for AIB1 (siAIB1), luciferase (siLUC), or no RNA (mock) as controls. Cells were harvested 48 hr after transfection. Downregulation of AIB1 expression was confirmed by real-time PCR (**A**) and Western blot (**B**).

C: IGF-I mRNA levels were determined by real-time PCR.

D: The percentage of apoptotic cells was determined by flow cytometry, after staining of cells with propidium iodide.

E: TUNEL assay showing apoptotic cells.

(Cardiff et al., 2000). This is also true for the lesions detected in our model, given that ∼50% of all aging animals developed one or more mammary tumors. Taken together, the mammary gland phenotype developed in AIB1-tg mice suggests that AIB1 is sufficient to trigger initial steps of tumor formation that ultimately lead to invasive carcinoma.

The AIB1-tg mice in this study showed a dramatic tumor incidence, with ∼76% of aging animals developing one or more tumors. In addition to mammary tumors, tumors were found in several other organs, including pituitary, lung, and uterus. All tumors developed in a focal and stochastic fashion. The frequency of mammary tumors and the stochastic appearance of tumors are comparable to many other tumor models using MMTV-driven oncogenes as transgenes (Cardiff and Muller, 1993). However, in contrast to other mouse models using MMTV-driven oncogenes, the tumors observed in AIB1-tg mice were surprisingly heterogeneous in type and organ distribution. This could be due to the somewhat altered expression pattern of the MMTV-AIB1 transgene as compared to other MMTV-driven transgenes (as discussed above).

Mammary adenocarcinomas in our study did not show a distinct "signature phenotype," but were of several subtypes, as defined by the Annapolis Panel (Cardiff et al., 2000), including acinar (also found in wnt-1 tgs), cribriform (as in c-*myc* tgs), and papillary (as in wnt-2 tg). In addition to mammary adenocarcinomas that are frequently found with other MMTV-driven oncogenes, tumors originating from cells other than epithelial cells were identified, including leiomyosarcomas, fibrosarcomas, teratomas, and papillomas. Consistent with the notion that AIB1 was the causative agent of these tumors, all tumors analyzed were AIB1-positive, and high levels of AIB1 expression were also detected in the respective tumor-free organ. Together, these findings raise the possibility that AIB1 may be involved in a much wider range of human tumors than previously thought.

After having established that AIB1 is a potent oncogene, we next wanted to determine the mechanism(s) of AIB1 oncogenicity. Several features of the observed phenotype suggested to us an involvement of the PI3K/AKT/mTOR pathway and its downstream targets (Bai et al., 2000; Mills et al., 2001; Hanahan and Weinberg, 2000). First, mammary glands and epithelial cells in AIB1-tgs showed an increased size as compared to wt mice, and the PI3K/AKT pathway has been implicated in the regulation of organ and cell size (Gingras et al., 2001).

Second, the histopathology of the premalignant lesions and mammary adenocarcinomas showed similarity to mouse models targeting members of the PI3K/AKT/mTOR signaling pathway. The unusual squamous metaplasia reported here strongly resembles the lesions found in β-catenin tg mice (Miyoshi et al., 2002). The precocious lobulo-alveolar development of the AIB1-tg mammary glands resembles that of mice engineered with a conditional loss of PTEN in the mammary gland (Li et al., 2002). The adenosquamous carcinomas and papillary and cribriform adenocarcinomas found in AIB1 transgenics have also been reported for cyclin D1 transgenics (Wang et al., 1994). Cyclin D1, β-catenin, and PTEN are all part of the PI3K/AKT/mTOR signaling pathway, a pathway increasingly linked to cancer (Scheid and Woodgett, 2001; Vivanco and Sawyers, 2002; Surmacz, 2003).

Our results demonstrate that the ectopic expression of AIB1 in the mammary gland leads to activation of several members of the IGF-IR/PI3K/AKT/mTOR pathway in primary mammary epithelial cell cultures, in whole mammary glands, and in primary mammary tumors. We also demonstrate a direct correlation between AIB1 expression levels and PI3K/AKT activation, since mouse strains or samples with higher AIB1 levels show increased activation of the pathway. Interestingly, we also found that other mouse models with activated PI3K/AKT pathway, namely TSC null mutants (not shown) and PTEN null mutants (Figure 7A), in turn show overexpression of pCIP (murine AIB1), suggesting that the activation of the PI3K/AKT pathway in

TSC$^{-/-}$ and PTEN$^{-/-}$ cells activates expression of the (endogenous) p/CIP gene. These findings indicate not only that AIB1 is sufficient to activate PI3K/AKT signaling, but also that it may be a target of this pathway through an autoregulatory feedback loop.

In an attempt to account for the increased IGF-IR activation in AIB1-tg mice, we further demonstrate an increase of IGF-I serum levels and IGF-I mRNA levels in mammary gland epithelial cells. These results indicate that AIB1 can modulate IGF-IR signaling in mammary epithelial cells in an endocrine and autocrine manner. Consistent with our findings, mice homozygous for a p/CIP null mutant display decreased serum levels of IGF-I and show dwarfism (Wang et al., 2000). Thus, regulation of IGF-I levels is not only a feature of the overexpressed, human AIB1 gene product, but can also be mediated by the endogenous gene.

It has been previously shown that in liver cells, the IGF-I promoter can be induced by estradiol. While this promoter does not contain a classical estrogen response element, ERα has been shown to act through an AP1 site (Umayahara et al., 1994). Since AIB1 acts as an ER coactivator, these findings suggest a direct mechanism for AIB1-mediated regulation of IGF-I levels and activation of the IGF-IR/PI3K/AKT/mTOR pathway. A direct involvement of AIB1 in the regulation of IGF expression is further demonstrated by our experiments showing that downregulation of AIB1 expression levels by RNA interference leads to reductions in IGF-I mRNA levels and a marked increase in apoptosis in primary epithelial and tumor cells. In addition, these results indicate that the survival of tumor cells from AIB1-tgs remains dependent on high-level AIB1 expression and therefore argue against the possibility that AIB1 might be only required for the induction of the premalignant phenotype observed in AIB1-tg animals but not for the generation of subsequent tumors.

Of note, serum IGF-I levels and IGF-IR signaling have been implicated in the etiology of breast cancer (LeRoith and Roberts, 2003), and IGF-IR signals synergize with ERα action in the regulation of proliferation and apoptosis (Dupont et al., 2000). IGF-I tgs have also been reported to display a high frequency (50%) of mammary tumors, albeit at a later onset (24 month) than in our study (Hadsell and Abdel-Fattah, 2001). Together, our data demonstrate a further connection between mammary tumor formation and the actions of ERα and IGF-I, as the estrogen receptor coactivator AIB1 is critically involved in the regulation of autocrine and systemic IGF-I levels.

At this point, we cannot rule out that other receptors and/or signaling pathways are also activated by AIB1, especially in non-mammary gland tumors and ERα negative mammary tumors, which await further investigation.

Taken together, our data establish that AIB1 can function as an oncogene and that the AIB1-tg mice produced in this study provide a useful model to study the progression from a premalignant mammary gland phenotype to malignant carcinomas. Furthermore, our data imply that the AIB1 gene amplification and overexpression observed in human breast cancer is a causal factor in the formation and progression of this disease and thus a potential drug target. Lastly, the AIB1-tg model will allow the dissection of the ERα-dependent and ERα-independent functions of AIB1 in mammary tumorigenesis, and points to a potential involvement of AIB1 in tumors of other organs that are not under estrogen control.

Experimental procedures

Generation of AIB1-tg mice
A 4.8 kb fragment of the human AIB1 cDNA (Anzick et al., 1997), kindly provided by Paul S. Meltzer, was isolated from the pcDNA3.1 AIB1 plasmid using ApaI and NotI restriction enzymes. A NotI site was added at the ApaI site. The fragment was cloned into the NotI site of the pTLMTV-SV40 vector (Muller et al., 1990), kindly provided by Dr. Philip Leder. To derive tg mice, the pTLMTVB-hAIB1 NheI/SalI fragment was microinjected into fertilized eggs derived from FVB/N mice as described (Muller et al., 1988). Mice were maintained on an FVB/N background using stock mice from Taconic Farms, Inc. Integration of the transgene into the offspring genome was assessed by Southern blot and PCR analysis.

RT-PCR and real-time PCR analysis
Total RNA from homogenized tissue samples was extracted by Trizol (Invitrogen), reverse transcribed, and amplified by PCR using the following primers: AIB1 sense: 5′GCTTGACATCCTTTGACTGG3′; AIB1 antisense: 5′TAAGATTGGCAGATATCAGCTCAGC3′; actin sense: 5′GGGTATGGAATCCTGTGGCA3′; actin antisense: 5′-TGGACAGTGAGGCCAAGATG3′. All real-time PCR reactions were performed using SYBR Green PCR Core Reagents kit (PE-Applied-Biosystem) and an ABI Prism 7700 sequence Detector System. Primers used for real-time PCR were: AIB1 sense, 5′GCGGCGAGTTTCCGATTTA3′; AIB1 antisense, 5′GCTCCCGTCTCCGTTTTTCT3′; p/CIP sense 5′ATTTGCTGAACAGTGGACTCC3′; p/CIP antisense 5′TTCGCCTAGTCCACTCATCCTG3′. IGF1 sense 5′GCTATGGCTCCAGCATTCG3′; IGF1 antisense 5′GCTCCGGAAGCAACACTCA3′; mouse GAPDH primers were obtained from Applied Biosystems.

Small interfering RNA transfection
100 nM of small interfering RNA (siRNA) duplex oligonucleotides (Dharmacon) targeting AIB1 mRNA (5′AGACUCCUUAGGACCGCUUdTdT3′) was transfected using Lipofectamine 2000 (Invitrogen) according to the manufacturer's instructions. Cells were harvested 48 hr after transfection.

Whole mounts, histology, and immunohistochemistry analysis
Mammary glands were dissected, mounted on glass slides, and stained as described at http://mammary.nih.gov/tools/histological/Histology/index.html. Tissues were fixed overnight in 10% neutralized buffered formalin and embedded in paraffin by standard procedures. Sections of 4 μm thickness were stained with H&E or processed for immunohistochemistry analysis following antigen retrieval. Polyclonal ERα (1:3000) (Santa Cruz) or polyclonal AIB1 (1:200) (produced in our laboratory) were routinely used. Slides were counterstained with hematoxylin.

BrdU labeling and TUNEL assays
Four hours before sacrifice, wt and tg mice at 2 weeks of pregnancy were injected with 20 μl/g of body weight of BrdU (Sigma). Cross-sections were stained with an anti BrdU antibody (BD Bioscience) and counterstained with hematoxylin. The number of BrdU-positive cells in wt and tg samples was counted in 10 fields per slide, under 20× magnification. Final results represent the average of 3 independently performed assays. TUNEL assays (Oncogene Research Products) were performed on cross-sections of mammary glands obtained from animals at day 4 of involution, according to the manufacturer's instructions.

Immunoblot analysis
Polyclonal rabbit anti-AIB1 antibody was produced in the lab, and used for Western blots and immunostaining. Goat anti-mouse IGF-I was obtained from Chemicon, polyclonal ERα rabbit (MC-20) from Santa Cruz. Polyclonal anti-Calnexin (Stressgen) was used as control for protein loading. All the antibodies for the PI3 kinase pathway were purchased from Cell Signaling Technology. Isolated mammary gland, tumor samples, or cells were lysed in ice-cold RIPA buffer including protease inhibitor cocktail (Roche). Lysates were centrifuged at 14,000 RPM for 15 min. 70 μg of protein was separated on 4%–15% SDS-PAGE gradient gel (Bio-Rad) and transferred to nitrocellulose membranes. Blots were probed with the antibodies indicated and developed with Renaissance chemiluminescent detection system (Perkin-Elmer).

Serum hormone measurements

Serum concentrations of prolactin (PRL), growth hormone (GH), and luteinizing hormone (LH) were measured using mouse PRL, GH, and LH radioimmunoassays by Dr. A.F. Parlow (National Hormone & Peptide Program Harbor-UCLA Medical Center), as described (Fedele et al., 2002).

Primary cell cultures

Tumor cells were isolated as described (Medina and Kittrell, 2000). Primary cultures of mouse mammary epithelium were prepared as described (Reginato et al., 2003).

Statistical analysis

Means and standard deviations have been estimated for continuous variables. Tumor-free survival was calculated using the product-limit method of Kaplan-Meier (Kaplan and Meier, 1958). Comparisons between subgroups of study mice and the significance of differences between survivals rates were ascertained using a two-sided log-rank test (Peto and Peto, 1972). Differences between the two populations were considered significant at confidence levels greater than 95% ($p < 0.05$).

References

Anzick, S.L., Kononen, J., Walker, R.L., Azorsa, D.O., Tanner, M.M., Guan, X.Y., Sauter, G., Kallioniemi, O.P., Trent, J.M., and Meltzer, P.S. (1997). AIB1, a steroid receptor coactivator amplified in breast and ovarian cancer. Science 277, 965–968.

Bai, J., Uehara, Y., and Montell, D.J. (2000). Regulation of invasive cell behavior by taiman, a Drosophila protein related to AIB1, a steroid receptor coactivator amplified in breast cancer. Cell 103, 1047–1058.

Bautista, S., Valles, H., Walker, R.L., Anzick, S., Zeillinger, R., Meltzer, P., and Theillet, C. (1998). In breast cancer, amplification of the steroid receptor coactivator gene AIB1 is correlated with estrogen and progesterone receptor positivity. Clin. Cancer Res. 4, 2925–2929.

Bouras, T., Southey, M.C., and Venter, D.J. (2001). Overexpression of the steroid receptor coactivator AIB1 in breast cancer correlates with the absence of estrogen and progesterone receptors and positivity for p53 and HER2/neu. Cancer Res. 61, 903–907.

Cardiff, R.D., and Muller, W.J. (1993). Transgenic mouse models of mammary tumorigenesis. Cancer Surv. 16, 97–113.

Cardiff, R.D., Anver, M.R., Gusterson, B.A., Hennighausen, L., Jensen, R.A., Merino, M.J., Rehm, S., Russo, J., Tavassoli, F.A., Wakefield, L.M., et al. (2000). The mammary pathology of genetically engineered mice: The consensus report and recommendations from the Annapolis meeting. Oncogene 19, 968–988.

Chen, H., Lin, R.J., Schiltz, R.L., Chakravarti, D., Nash, A., Nagy, L., Privalsky, M.L., Nakatani, Y., and Evans, R.M. (1997). Nuclear receptor coactivator

ACTR is a novel histone acetyltransferase and forms a multimeric activation complex with P/CAF and CBP/p300. Cell 90, 569–580.

Choi, Y.W., Henrard, D., Lee, I., and Ross, S.R. (1987). The mouse mammary tumor virus long terminal repeat directs expression in epithelial and lymphoid cells of different tissues in tg mice. J. Virol. 61, 3013–3019.

Conlon, I., and Raff, M. (1999). Size control in animal development. Cell 96, 235–244.

Cui, X., Lazard, Z., Zhang, P., Hopp, T.A., and Lee, A.V. (2003a). Progesterone crosstalks with insulin-like growth factor signaling in breast cancer cells via induction of insulin receptor substrate-2. Oncogene 22, 6937–6941.

Cui, X., Zhang, P., Deng, W., Oesterreich, S., Lu, Y., Mills, G.B., and Lee, A.V. (2003b). Insulin-like growth factor-I inhibits progesterone receptor expression in breast cancer cells via the phosphatidylinositol 3-kinase/Akt/ mammalian target of rapamycin pathway: Progesterone receptor as a potential indicator of growth factor activity in breast cancer. Mol. Endocrinol. 17, 575–588.

Dupont, J., Karas, M., and LeRoith, D. (2000). The potentiation of estrogen on insulin-like growth factor I action in MCF-7 human breast cancer cells includes cell cycle components. J. Biol. Chem. 275, 35893–35901.

Fedele, M., Battista, S., Kenyon, L., Baldassarre, G., Fidanza, V., Klein-Szanto, A.J., Parlow, A.F., Visone, R., Pierantoni, G.M., Outwater, E., et al. (2002). Overexpression of the HMGA2 gene in tg mice leads to the onset of pituitary adenomas. Oncogene 21, 3190–3198.

Font de Mora, J., and Brown, M. (2000). AIB1 is a conduit for kinase-mediated growth factor signaling to the estrogen receptor. Mol. Cell. Biol. 20, 5041–5047.

Gingras, A.C., Raught, B., and Sonenberg, N. (2001). Regulation of translation initiation by FRAP/mTOR. Genes Dev. 15, 807–826.

Glass, C.K., and Rosenfeld, M.G. (2000). The coregulator exchange in transcriptional functions of nuclear receptors. Genes Dev. 14, 121–141.

Gunzburg, W.H., and Salmons, B. (1992). Factors controlling the expression of mouse mammary tumour virus. Biochem. J. 283, 625–632.

Hadsell, D.L., and Abdel-Fattah, G. (2001). Regulation of cell apoptosis by insulin-like growth factor I. Adv. Exp. Med. Biol. 501, 79–85.

Halachmi, S., Marden, E., Martin, G., MacKay, H., Abbondanza, C., and Brown, M. (1994). Estrogen receptor-associated proteins: possible mediators of hormone-induced transcription. Science 264, 1455–1458.

Hanahan, D., and Weinberg, R.A. (2000). The hallmarks of cancer. Cell 100, 57–70.

Kaplan, E., and Meier, P. (1958). Non-parametric estimation for incomplete observation. J. Am. Stat. Assoc. 53, 457–471.

King, L.B., and Corley, R.B. (1990). Lipopolysaccharide and dexamethasone induce mouse mammary tumor proviral gene expression and differentiation in B lymphocytes through distinct regulatory pathways. Mol. Cell. Biol. 10, 4211–4220.

Leevers, S.J., Weinkove, D., MacDougall, L.K., Hafen, E., and Waterfield, M.D. (1996). The Drosophila phosphoinositide 3-kinase Dp110 promotes cell growth. EMBO J. 15, 6584–6594.

LeRoith, D., and Roberts, C.T., Jr. (2003). The insulin-like growth factor system and cancer. Cancer Lett. 195, 127–137.

Li, G., Robinson, G.W., Lesche, R., Martinez-Diaz, H., Jiang, Z., Rozengurt, N., Wagner, K.U., Wu, D.C., Lane, T.F., Liu, X., et al. (2002). Conditional loss of PTEN leads to precocious development and neoplasia in the mammary gland. Development 129, 4159–4170.

Liao, L., Kuang, S.Q., Yuan, Y., Gonzalez, S.M., O'Malley, B.W., and Xu, J. (2002). Molecular structure and biological function of the cancer-amplified nuclear receptor coactivator SRC-3/AIB1. J. Steroid Biochem. Mol. Biol. 83, 3–14.

List, H.J., Reiter, R., Singh, B., Wellstein, A., and Riegel, A.T. (2001). Expression of the nuclear coactivator AIB1 in normal and malignant breast tissue. Breast Cancer Res. Treat. 68, 21–28.

McKenna, N.J., Xu, J., Nawaz, Z., Tsai, S.Y., Tsai, M.J., and O'Malley, B.W. (1999). Nuclear receptor coactivators: Multiple enzymes, multiple complexes, multiple functions. J. Steroid Biochem. Mol. Biol. 69, 3–12.

Medina, D., and Kittrell, F. (2000). Establishment of mouse mammary cell lines. In Methods in Mammary Gland Biology and Breast Cancer Research, M.M. Ip and. B.B. Asch, eds. (Buffalo, NY: Kluwer Academic/Plenum publishers), pp. 137–145.

Mills, G.B., Lu, Y., Fang, X., Wang, H., Eder, A., Mao, M., Swaby, R., Cheng, K.W., Stokoe, D., Siminovitch, K., et al. (2001). The role of genetic abnormalities of PTEN and the phosphatidylinositol 3-kinase pathway in breast and ovarian tumorigenesis, prognosis, and therapy. Semin. Oncol. 28, 125–141.

Miyoshi, K., Shillingford, J.M., Le Provost, F., Gounari, F., Bronson, R., von Boehmer, H., Taketo, M.M., Cardiff, R.D., Hennighausen, L., and Khazaie, K. (2002). Activation of β-catenin signaling in differentiated mammary secretory cells induces transdifferentiation into epidermis and squamous metaplasias. Proc. Natl. Acad. Sci. USA 99, 219–224.

Muller, W.J., Sinn, E., Pattengale, P.K., Wallace, R., and Leder, P. (1988). Single-step induction of mammary adenocarcinoma in tg mice bearing the activated c-neu oncogene. Cell 54, 105–115.

Muller, W.J., Lee, F.S., Dickson, C., Peters, G., Pattengale, P., and Leder, P. (1990). The int-2 gene product acts as an epithelial growth factor in tg mice. EMBO J. 9, 907–913.

Munoz, B., and Bolander, F.F., Jr. (1989). Prolactin regulation of mouse mammary tumor virus (MMTV) expression in normal mouse mammary epithelium. Mol. Cell. Endocrinol. 62, 23–29.

Osborne, C.K., Bardou, V., Hopp, T.A., Chamness, G.C., Hilsenbeck, S.G., Fuqua, S.A., Wong, J., Allred, D.C., Clark, G.M., and Schiff, R. (2003). Role of the estrogen receptor coactivator AIB1 (SRC-3) and HER-2/neu in tamoxifen resistance in breast cancer. J. Natl. Cancer Inst. 95, 353–361.

Patel, S., Lochhead, P.A., Rena, G., Fumagalli, S., Pende, M., Kozma, S.C., Thomas, G., and Sutherland, C. (2002). Insulin regulation of insulin-like growth factor-binding protein-1 gene expression is dependent on the mammalian target of rapamycin, but independent of ribosomal S6 kinase activity. J. Biol. Chem. 277, 9889–9895.

Peto, R., and Peto, J. (1972). Asymptotically efficient rank invariant test procedures (with discussion). J. R. Stat. Soc. A. 135, 185–207.

Reginato, M.J., Mills, K.R., Paulus, J.K., Lynch, D.K., Sgroi, D.C., Debnath, J., Muthuswamy, S.K., and Brugge, J.S. (2003). Integrins and EGFR coordinately regulate the pro-apoptotic protein Bim to prevent anoikis. Nat. Cell Biol. 5, 733–740.

Sakakura, C., Hagiwara, A., Yasuoka, R., Fujita, Y., Nakanishi, M., Masuda, K., Kimura, A., Nakamura, Y., Inazawa, J., Abe, T., and Yamagishi, H. (2000). Amplification and over-expression of the AIB1 nuclear receptor co-activator gene in primary gastric cancers. Int. J. Cancer 89, 217–223.

Scheid, M.P., and Woodgett, J.R. (2001). Phosphatidylinositol 3′ kinase signaling in mammary tumorigenesis. J. Mammary Gland Biol. Neoplasia 6, 83–99.

Scheinman, R.I., Cogswell, P.C., Lofquist, A.K., and Baldwin, A.S., Jr. (1995). Role of transcriptional activation of IκBα in mediation of immunosuppression by glucocorticoids. Science 270, 283–286.

Shang, Y., Hu, X., DiRenzo, J., Lazar, M.A., and Brown, M. (2000). Cofactor dynamics and sufficiency in estrogen receptor-regulated transcription. Cell 103, 843–852.

Suen, C.S., Berrodin, T.J., Mastroeni, R., Cheskis, B.J., Lyttle, C.R., and Frail, D.E. (1998). A transcriptional coactivator, steroid receptor coactivator-3, selectively augments steroid receptor transcriptional activity. J. Biol. Chem. 273, 27645–27653.

Surmacz, E. (2003). Growth factor receptors as therapeutic targets: Strategies to inhibit the insulin-like growth factor I receptor. Oncogene 22, 6589–6597.

Takeshita, A., Cardona, G.R., Koibuchi, N., Suen, C.S., and Chin, W.W. (1997). TRAM-1, A novel 160-kDa thyroid hormone receptor activator molecule, exhibits distinct properties from steroid receptor coactivator-1. J. Biol. Chem. 272, 27629–27634.

Torchia, J., Rose, D.W., Inostroza, J., Kamei, Y., Westin, S., Glass, C.K., and Rosenfeld, M.G. (1997). The transcriptional co-activator p/CIP binds CBP and mediates nuclear-receptor function. Nature 387, 677–684.

Umayahara, Y., Kawamori, R., Watada, H., Imano, E., Iwama, N., Morishima, T., Yamasaki, Y., Kajimoto, Y., and Kamada, T. (1994). Estrogen regulation of the insulin-like growth factor I gene transcription involves an AP-1 enhancer. J. Biol. Chem. 269, 16433–16442.

Vivanco, I., and Sawyers, C.L. (2002). The phosphatidylinositol 3-kinase AKT pathway in human cancer. Nat. Rev. Cancer 2, 489–501.

Wakefield, L.M., Thordarson, G., Nieto, A.I., Shyamala, G., Galvez, J.J., Anver, M.R., and Cardiff, R.D. (2003). Spontaneous pituitary abnormalities and mammary hyperplasia in FVB/NCr mice: implications for mouse modeling. Comp. Med. 53, 424–432.

Wang, T.C., Cardiff, R.D., Zukerberg, L., Lees, E., Arnold, A., and Schmidt, E.V. (1994). Mammary hyperplasia and carcinoma in MMTV-cyclin D1 transgenic mice. Nature 369, 669–671.

Wang, Z., Rose, D.W., Hermanson, O., Liu, F., Herman, T., Wu, W., Szeto, D., Gleiberman, A., Krones, A., Pratt, K., et al. (2000). Regulation of somatic growth by the p160 coactivator p/CIP. Proc. Natl. Acad. Sci. USA 97, 13549–13554.

Wang, Y., Wu, M.C., Sham, J.S., Zhang, W., Wu, W.Q., and Guan, X.Y. (2002). Prognostic significance of c-myc and AIB1 amplification in hepatocellular carcinoma. A broad survey using high-throughput tissue microarray. Cancer 95, 2346–2352.

Werbajh, S., Nojek, I., Lanz, R., and Costas, M.A. (2000). RAC-3 is a NF-κB coactivator. FEBS Lett. 485, 195–199.

Wu, R.C., Qin, J., Hashimoto, Y., Wong, J., Xu, J., Tsai, S.Y., Tsai, M.J., and O'Malley, B.W. (2002). Regulation of SRC-3 (pCIP/ACTR/AIB-1/RAC-3/TRAM-1) Coactivator activity by IκB kinase. Mol. Cell. Biol. 22, 3549–3561.

Xu, J., Qiu, Y., DeMayo, F.J., Tsai, S.Y., Tsai, M.J., and O'Malley, B.W. (1998). Partial hormone resistance in mice with disruption of the steroid receptor coactivator-1 (SRC-1) gene. Science 279, 1922–1925.

Xu, J., Liao, L., Ning, G., Yoshida-Komiya, H., Deng, C., and O'Malley, B.W. (2000). The steroid receptor coactivator SRC-3 (p/CIP/RAC3/AIB1/ACTR/TRAM-1) is required for normal growth, puberty, female reproductive function, and mammary gland development. Proc. Natl. Acad. Sci. USA 97, 6379–6384.